An Overview of the Impedance Models of the Thorax and the Origin of the Impedance Cardiography Signal for Modelling of the Impedance Signals

Yar M. Mughal, Jr-*EMBS Member, IEEE Member*, Paul Annus, *IEEE Member*, Mart Min, *Senior IEEE Member* and Rauno Gordon

***Abstract*—This paper presents our work in the search for a realistic thorax impedance model that is suitable for the simulation of an impedance cardiography (ICG) signal model. The developed ICG signal model would be useful to evaluate the performance of e.g. algorithms for the separation of cardiac and respiratory signals. Five different impedance models of the thorax were studied to evaluate their suitability with respect to the development of the ICG signal model. We found out that none of the models would be accurate enough to imitate the real human thorax phenomena in the context of ICG. In addition, we also reviewed the generation of (bio-) impedance signal in order to understand the origin of the ICG signal waveform. It is found that although a consensus exists in the scientific community, several researchers have expressed doubts about the generally admitted origin of impedance signal waveform. The present study concludes that the ICG signal model could be mathematically derived from measured electrical bio-impedance (EBI) data obtained with a specific electrodes configuration.**

I. Introduction

The measurement of thoracic electrical impedance has been practiced since the 1930s. As a measurement technique, the impedance method is generally viewed as a promising non-invasive method for measuring cardiac output (CO) [1] and other physiological and biological parameters.

Nevertheless, the anatomical structure of the human thorax is very complex and its electrical properties are related to anisotropic and inhomogeneous structures in it [2].

The formation of the ICG waveform is essential for understanding the physiological activities and anatomy of the human thorax as well as the origin of the ICG signal. In the formation of the impedance signal, each organ and tissue makes its contribution [3]. Several methods have been used to understand the origin of the ICG signal [4] and relate it to physiological activities. The main obstacle in cardiovascular impedance measurement is the incapability to precisely associate the measured impedance waveforms to the original mechanical and physiological activities of the heart and following blood volume changes (ΔBV) happening in it [3].

This research was supported by the European Union through the European Regional Development Funding in the frames of the research center CEBE and the competence center ELIKO, the Estonian Ministry of Education and Research (Institutional Research Project IUT19-11) the Found. Archimedes ESF DoRa and Estonian Science Found. Grant (9394).

Y. M. Mughal, P. Annus, M. Min and R. Gordon are with Thomas Johann Seebeck Department of Electronics, Tallinn University of Technology, Ehitajate tee 5, Tallinn, Estonia. (email: yar@elin.ttu.ee phone: +37258026086) and also with the competence center ELIKO.

In order to determine the variations from basal impedance (Z_0), one can detect the resistivity variations in the thorax (or construct a model of it) from the potential of the ICG leads field that can be obtained by changing the conductivity values of the thorax or constructed model [3].

This study focuses on the selection of a thorax impedance model suitable for generating an ICG signal model. In principle, the signal model development could be based on existing selected thorax impedance model or measured electrical bio-impedance (EBI) data.

In this paper, five thorax impedance models and the origin of the ICG signal waveforms are discussed with respect to the ICG signal model development.

Such ICG signal model could be used to evaluate the performance of e.g. algorithms for the separation of cardiac and respiratory signals instead of relying on measured EBI data, which have been shown to be impractical [5].

II. Impedance Models Of The Thorax

The existing impedance models vary from the simplest (e.g. two or more compartments) ones to the 3D model of the thorax. They were studied to evaluate their suitability for developing a realistic ICG signal model that is as accurate as possible.

A. Simplified Model of the Thorax

This is a very simplified thorax model in which the thorax is considered to be divisible into two parts: tissue (A_t) and fluids (A_b). The parts are characterized by area A of the cross-section of each, as depicted in Fig. 1. This model was developed to find the relationship between change in blood volume (ΔBV) and impedance change (ΔZ). The following equation was found to describe this relationship [2]:

$$dv_b = \rho_b l^2 / Z^2 dZ \qquad (1)$$

where d_{vb} is the change of blood volume, ρ_b is the resistivity of blood, l is the distance between the measurement electrodes, Z is the thorax impedance, and dZ is the impedance change.

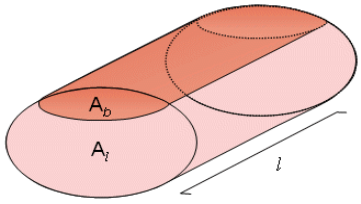

Figure 1. A simple thorax's cylindrical model, which contains a uniformly distributed blood and tissue compartments for determining the net torso impedance [2].

B. *Ideal Cylindrical Models*

The cylindrical models can have one- or two-compartments. The one- and two- compartment cylinder models are depicted in Fig 2(a-b). The cross sectional area of the ideal cylinder models may be elliptic, circular, or could have any plane [6].

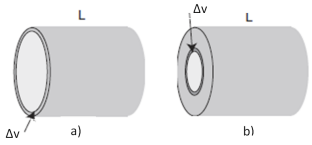

Figure 2. Ideal Cylindrical Models [6]:
a) One-compartment cylinder model, b) Two-compartment cylinder model

In the simple cylindrical model, the thorax is divided into either one or two compartments with the same resistivity. In Fig. 2, L is the length and Δv is the parallel volume increment such that:

$$\Delta/ = \Delta v/v \qquad (2)$$

Equation (2) is for one compartment (Fig 2a). It is clear that the relative ΔBV can be found without knowing the dimensions of the cylinder:

$$\Delta/ = \Delta v/\Delta v + v_A + v_t \qquad (3)$$

In the two-compartment model (Fig 2b), the two cylinders are physically in parallel and the conductance model preferred where $\Delta v+v_A$ is the volume of the inner cylinder, and v_t is the volume of the outer cylinder. Equation (3) shows that the sensitivity decreases with a larger surrounding volume (v_t) [6].

C. *Kinnen's Thorax Model*

Kinnen et al. developed their model based on a cylindrical thorax model [2]. The purpose of this model is to examine the generation of the impedance signal. The model is depicted in Fig. 3, in which the thorax model is divided into two cylindrical parts. The inner part of the model characterizes the BV of the heart and primary arteriovenous system of the thorax. The lungs are characterized by the medium outside the inner part. The resistance for the inner part of the model was taken equal to 495 Ω, and 32 Ω for the other part.

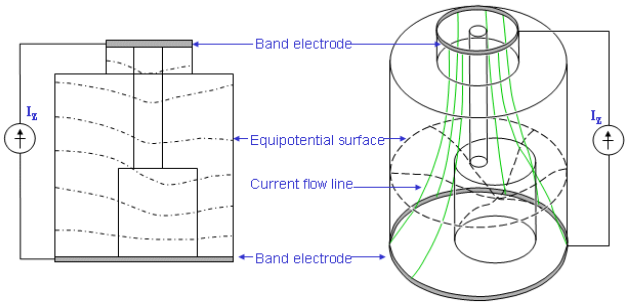

Figure 3. Kinnen's Thorax Model [2]

D. *Sakamoto's Thorax Model*

Sakamoto et al. [7] developed a model that is anatomically more realistic. This model consists of the heart, aorta, lungs, vena cava and torso shape, as depicted in Fig. 4 (b-c). The model allows investigating the effect of conductivity variations of the tissues on the measured impedance. These results showed that the information connected to the blood circulation in the human thorax could be measured by potential distribution changes on the body surface.

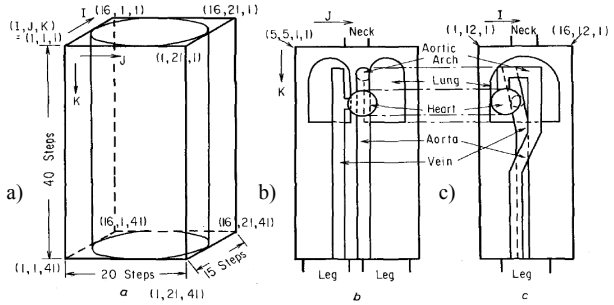

Figure 4. Simplified Sakamoto's thorax model:
a) model of human body, b) cross-section at I=5,5, c) cross-section at J=12 [7].

The impedance waveform is affected not only by the CO or the ΔBV in the aorta, but also by the ΔBV in the heart and lungs [7].

In Fig. 5, the solid lines depict the impedance signal waveform ΔZ, which is recorded through different pairs of point electrodes around the human thorax, and the dotted line represents the signal waveform recorded through the pair of band electrodes. This impedance signal waveform is affected through the ΔBV in both the heart and the aorta [7].

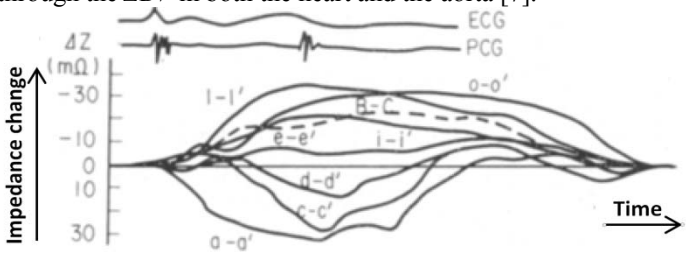

Figure 5. Impedance signal recorded by different pairs of point and band electrodes around the thorax [7].

E. *3-D Thorax Model*

The 3-D thorax model is composed of lungs, muscle, heart and spinal column, as depicted in Fig. 6. The potential distribution can reflect different effects when inhaling (Fig. 6(a)) and exhaling (Fig. 6(b)); the lungs become smaller when exhaling and larger when inhaling. The potential distribution fluctuates with the change of resistivities caused by the activities in the thorax, for example, inspiration and expiration (cf. Fig. 7). Thus, the model is helpful to judge whether there are more or less physiological activities or pathologic variations in the studied subject [8].

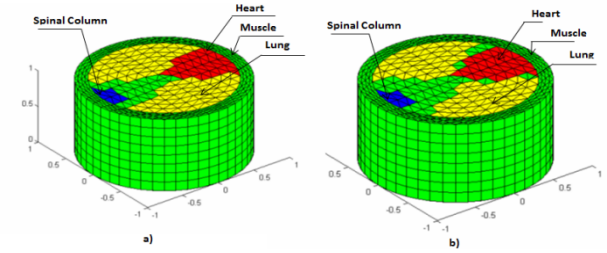

Figure 6. 3D thorax model at the end of phase: a) inhaling b) exhaling [8]

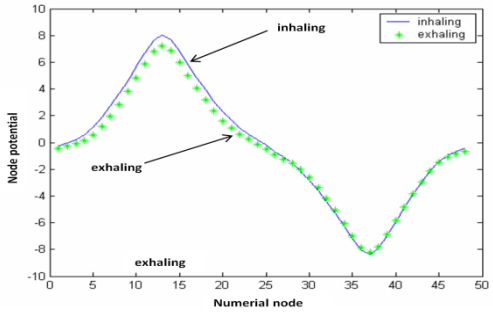

Figure 7. Changing of the node potentials during haling [8].

III. Origin of The ICG Signal

This section reviews the history of the ICG signal origin generation; understanding and waveform markers are discussed. In particular, it is found that although there exists a consensus within the scientist community, doubts and critical analyses about the origin of ICG signal have been expressed.

A. Analysis of Original ICG Signal Waveform

A typical impedance signal (*ΔZ*) and its first derivative (*dZ/dt*) can give detailed information about the physiological activities of thorax. Fig. 8 [9] depicts the different marks on the waveform which indicate the important points. The corresponding ECG is also depicted in Fig. 8. Research efforts have focused on discovering the physiological correlation with the ICG signal and its origin. It has been studied together with its first derivative [1, 36].

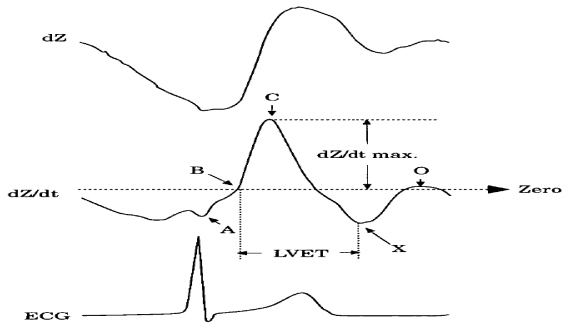

Figure 8. Characteristic impedance (*dZ*) signal, first derivative (*dZ/dt*) of impedance signal and ECG signal [1].

In 1970, Karnegis and Kubicek first indicated that the A-wave of the *dZ/dt* is associated with the P-wave of the ECG and that the C-wave of *dZ/dt* is associated with ventricular contractions [9]. During diastole, it was noticed another upward deflection of the O-wave in the *dZ/dt* signal. During the study, they found that the B point of *dZ/dt* corresponds to the aortic valve opening and the X point to the aortic valve closure. Several researchers make use of echocardiography and aortic pressure recordings and have confirmed these observations.

Furthermore, studies are required to confirm the exact physiological and anatomical origin of the impedance cardiography signal. Several investigators have dealt with this topic in the past, including a modelling and study performed on animals [1].

Witso & Kottke conducted these experiments in 1967 with dogs, using venous occlusion achieved by inflated ball [10].

Baker et al. reported experimental results in 1974. During their experiment, the ventricles were operated either at the same time or individually. From the experiment, it is concluded that the contribution of the left ventricle (LV) to the impedance signal waveform was 62% of the total impedance signal; on the other hand, the contribution from the right ventricle (RV) was 38% [11].

Kubicek et al. concluded in 1974 that the systolic portion of the *dZ/dt* impedance signal waveform was mainly contributed to by left ventricle ejection (LVE) into the aorta [12]. However, Thompson and Joekes reported in 1981 that both sides of the heart, left and right, make a main contribution to the systolic *dZ/dt* impedance signal waveform [13]. Wang et al. in 1991 presented that the impedance signal waveform was perhaps related to the right heart instead of left heart [14].

In 1979 Sakamoto proposed that the contribution of the BV variation in the lungs was very small [7], although Patterson in 1985 suggested that the lungs were one of the two largest origin source of the impedance signal waveform [15].

In 1979, Sakamoto and Kania reported that another possible reason of the impedance variations is resistivity change of the subsequent blood caused by a preferred orientation of the red blood cell [16].

Sakamoto et al. in 1979 and Lemberts et al. in 1984 point out that the blood resistivity change in the main arteries and veins contributed approximately one half to the overall *ΔZ* signal [16], [17]. The movement of the thoracic organ may also be a contributor to the impedance change [7].

In 1981, Mohapatra conducted a critical analysis on several of the hypotheses regarding the origin of the cardiac impedance signal waveform. In this study, he concluded that the signal is due to cardiac hemodynamics only. Moreover, the impedance signal reflects both changes in the blood velocity as well as changes in blood volume (ΔBV). The changing speed of forcing out affects the systolic behaviour of *ΔZ*, while changing volume (mostly of the atria and great veins) affects the diastolic portion of the impedance signal waveform curve [18].

In 1986, Penney concludes several studies which are based on the observations of contributions to the impedance signal waveform; his findings are reported in Table I [19].

TABLE I. Origin of The Impedance Signal in ICG [19]

Tissue/Organ	Contribution in %
Aorta and thoracic musculature	+60%
Pulmonary artery & lungs	+60%
Vena cava and right atrium	+20%
Pulmonary vein and left atrium	+20%
Left ventricle	-30%
Right ventricle	-30%

In 1988, Mohapatra reported in his critical analysis that the evidence that the impedance plethysmography is at the origin of the impedance signal is very weak; but this is not exactly known until now [20]. In 1995, Wang and Patterson reported that the exact origin(s) or a region in the thorax that causes the impedance change during cardiac cycle, are unknown. It is suggested that contributions from many regions or origins invest to the formation of the impedance change [21].

Later, Kauppinen et al., as well as Patterson, reported controversial research findings. In 1998, Kauppinen et al. reported results that state that it is likely that more than 55% of the time-varying signal originates from the skeletal muscle even though that amount of measurement sensitivity originates in it. The contribution from the ventricle, aortas, carotid artery and jugular vein in 4 cases was 3.06%, 2.36%, 3.66% and 3.39%, respectively [3]. The obtained results also confirm the reported measurement problem when using sternal electrode for impedance cardiography [22].

In 2010, Patterson reported new controversial results: the aorta is a very weak contributor to the source of the impedance signal. The aorta contributes approximate only 1% to the total impedance measurement [23]. These reported results are closely agreeing with that of Kauppinen et al. [3]. The comparisons of contribution of tissues/organs are shown in Table II.

TABLE II. IMPEDANCE CONTRIBUTION FROM EACH TISSUE [3], [23].

Tissue/Organ	Kauppinen et al 1998	Patterson 2010
Skeletal muscle	67.00%	52.90%
Left lung	4.64%	3.17%
Right lung	4.15%	3.48%
Liver	1.59%	3.62%
Aortic arch/Aorta	0.26%	0.89%
Others	22.36%	35.94%
Total	100.00%	100.00%

Both studies reported the large contribution of the skeletal muscle to total impedance signal and a small contribution by the aorta in impedance waveform.

B. Waveform Markers

Waveform markers are the physiological indicators of different activities (see Fig. 8) [1]. The B waveform marker is the standard B points for the ICG waveform [36].

1) The A-wave marker

A wave associates with the contraction of atria, as found by Karnegis et al. [9] and others who found undoubted evidence. The hypothesis rose that the source of the A-wave marker is due to the back flow of blood from the atria into central veins. The A-wave marker is depicted in Fig. 8.

In 1979, Takada et al. found evidence that the left atrium might be the major contributor to this wave [24]. However, the exact contributions of the right and left atria are not known [1].

2) The C-wave marker

Several studies have taken place to unravel the origin of the systolic C-wave in the impedance cardiogram, since the absolute height (dZ/dt_{max}), depicted in Fig. 8, is used to calculate stroke volume (SV). These studies took place on animals and models by several researchers using different approaches, such as described in [17, 25, 26, 27, 28, 29, 30, 31 and 32].

In order to unravel a more elaborate explanation of the origin of the C-wave marker, researchers have attempted to imitate impedance cardiographic variations in a model. Still, these are far from reliable evidence, and most fail to give details of the relationship between dZ/dt_{max} and other physiological variables as aortic peak flow velocity. More study is required on the contributors to dZ/dt_{max} as predicted by a model [1].

3) The O-wave marker

The O-wave marker corresponds to the diastolic upward deflection of the *dZ/dt* signal, which is depicted in Fig. 8. In 1970, Lababidi Ehmke and Rurnin published their findings and many researchers prove its origin, which is described in [33].

IV. DEVELOPMENT OF THE TARGETED ICG MODEL

Based on the literature survey and analysis of the existing thorax impedance models and origin of the ICG signal, it can be concluded that none of these models are accurate enough to imitate the real phenomena in the ICG signal. A summary and the limitations of each model are discussed in Table III.

TABLE III. SUMMARY AND LIMITATION OF EXISTING MODELS

Model	Summary and limitations
Simplified Model of Thorax	This thorax model is highly simplified since the division into only two uniform tissues is used and geometrically it is not realistic. On the contrary, the real structure of the human thorax is very complicated.
Ideal Cylindrical Model	This model is also very simple because a simple cylinder is used to represent the thorax structure. In particular, the cross sectional point of view is not taken into account.
Kinnen's Thorax Model	Kinnen's model is simple; it indicates only two conductivity zones (blood volume of heart & primary arteriovenous system, and lungs). Most of the current flow would pass by the lungs. In this case, the generation of the impedance signal waveforms is primarily based on right ventrical (RV), which is not true if we consider the real thorax physiology.
Sakamoto's Thorax Model	This is not an accurate enough thorax impedance model because the blood pumps more toward the left leg side.
3-D Thorax Model	The model is not accurate enough because it uses a cylinder as the structure of the thorax. Furthermore, it does not take the variation of heart size during inhaling and exhaling into account.

Given these limitations, it is thus decided to use a sixteen electrodes' configuration belt to measure the ICG signal instead of the above models. Such a type of electrodes' setup is presumed to allow raising strong enough variations of the EBI in order to record the cardiac and respiration signals, which are caused by the heart and lungs. Further details about the EBI measurement setup can be found in [34].

The curve fitting method is used to develop an ICG signal model. With this approach, the ICG signal model would be more realistic and the underlying model parameters could be easily tuneable.

The EBI measurement procedure and the models and evaluation methods are discussed below.

A. EBI Measurement Procedure

The impedance measurement system consists of sixteen active electrodes; each of them can be used for measurement as well as excitation. The electrodes are connected to the impedance analyzer using a switch-box that can cross-switch any of the 16 electrode-inputs to any of the four analyzer-outputs, which is depicted in Fig. 9.

Figure 9. Switchbox with four capacitive and four active electrodes are attached

The datasets were obtained using multiple pairs of electrodes with four different positioning of the electrodes. The electrode setup is used for EBI measurement, which is shown in Fig. 10.

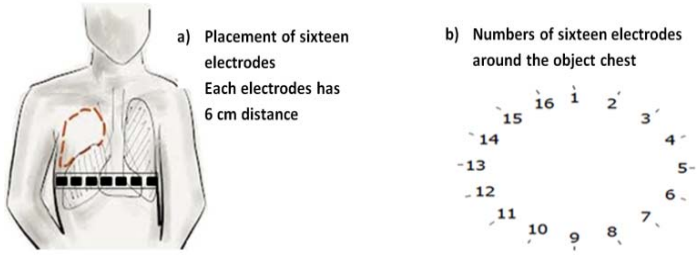

Figure 10. Sixteen electrodes configured belt, which is used for the EBI measurement procedure [34].

The measured datasets are obtained from a healthy male subject aged between 40 and 50 years, in a seated position.

The total EBI dataset was divided into three different segments. Each segment contains 10 seconds of the total EBI raw data, about 10,000 samples. Accordingly, the structure of the three segments is as follows:

a) cardiac only (breathing was held),
b) cardiac + respiration (deep breathing),
c) cardiac + respiration + motion artefacts (normal breathing with added motion artefacts).

In what follows, the four ICG datasets correspond to b) and the clean ICG and IRG datasets correspond to filtered versions of a) and b), respectively.

In Fig. 11 (Datasets 1-6), each dataset has been measured from different positioning of electrodes.

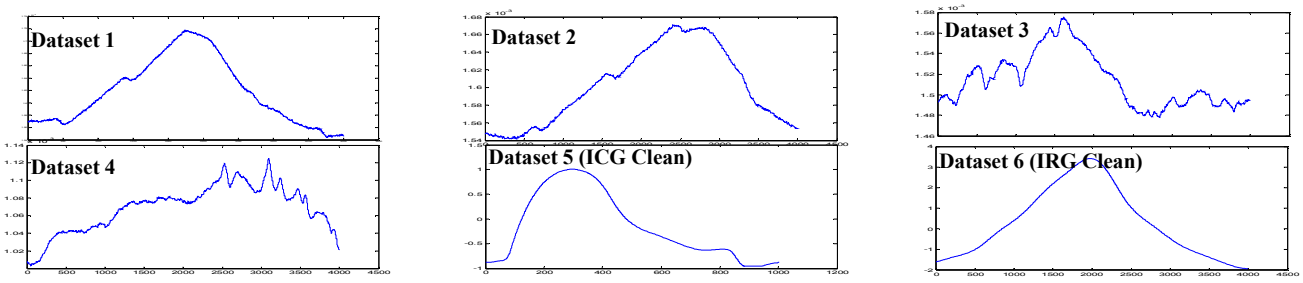

Figure 11. Measured EBI datasets with different configuration of electrodes.

B. Models and Evaluation Methods

Different curve fitting methods such as polynomial with different orders, Fourier series and sum of sine with different terms have been evaluated. The best-fit model performance has been selected based on the Sum Square Error (SSE), correlation (R-square) and execution time. Further details can be found in [35].

1) Polynomial Model

Polynomials are well suited for cases where a fairly simple empirical model is needed; the general polynomial model formula is given in Equation 4:

$$y = \sum_{i=1}^{n+1} p_i t^{n+1-i} \quad (4)$$

where n is the degree of the polynomial (highest power of the predictor variable), $n+1$ is the order of the polynomial (number of coefficients), p_i are the coefficients and t is time.

2) Fourier Series Model

The Fourier series is a sum of sine and cosine functions that describes a periodic signal. The model formula is given in Eq. 5:

$$y = a_0 + \sum_{i=1}^{n} a_i \cos(i\omega t) + b_i \sin(i\omega t) \quad (5)$$

where a_0 is the intercept, which is constant term in the data, ω is the fundamental frequency and n is the number of terms in the series.

3) Sum of Sine Waves Model

This model consists of a sum of sine terms only. The model formula is given in Equation 6:

$$y = \sum_{i=1}^{n} a_i \sin(i\omega t + c_i) \quad (6)$$

where a is the amplitude, ω is the frequency, c the phase, which is constant for each term and n is the total terms in series.

V. Discussion, Conclusion and Future Work

It is concluded that the simplified, Ideal Cylindrical, and Kinnen's models are too simple models that only take a few basic parameters into account. Sakamoto's and the 3-D model are more advanced and closer to reality, but still not accurate enough to imitate the complicated structure of the human thorax and different electrical properties of tissues such as anisotropy and inhomogeneity. Thus, we consider that none of these models is complete enough for developing the targeted ICG signal model.

Based on the reviewed existing thorax models and controversial statements regarding the origin of the impedance signal, we have started to evaluate how measured electrical bioimpedance (EBI) data can be used to develop an ICG signal model which closely imitates the real phenomena.

For this, we have built upon our previous study in which the EBI data was measured through a sixteen electrodes configuration belt from a normal human thorax [34]. The various curve-fitting methods have been used to process the collected data and in turn derive a mathematical model of the ICG signal. A practical application of this work can be found in [35] where a Bio-Impedance Signal Simulator (BISS) is described and implemented.

In future work, we will further investigate the modelling of the relation between cardiac and respiratory signals depending on human activity and health condition.

Acknowledgment

The authors thank Prof. T. Rang, Dr. T. Parve, Dr. Y. Le Moullec, Dr. A. Krivoshei and M. Rist for providing valuable advice. The authors are associated with, and all work has been done at, Th. J. Seebeck Dept. of Electronics, Tallinn University of Tech. and competence center ELIKO, Estonia.

This research was supported by the European Union through the European Regional Development Funding in the frames of the research center CEBE and the competence center ELIKO, the Estonian Ministry of Education and Research (IUT19-11), Foundation Archimedes ESF DoRa program and Estonian Science Foundation (9394).

References

[1] H. Woltjer, H. Bogaard, and P. Vries, "The technique of impedance cardiography, " European Heart Journal, vol. 18, pp1396-1403, 1997.

[2] J. Malmivuo and R. Plonsey, Bioelectromagnetism - Principles & Appl. of Bioelectric and Biomagnetic Fields, NY, Oxford Univ. Press, 1995.

[3] P. Kauppinen, J. Hyttinen and J. Malmivuo, "Sensitivity Distribution of Impedance Cardiography Using Band and Spot Electrodes Analyzed by a Three-Dimenional Computer Model", Annals of Biomedical Engineering Vol. 26, 694-702. 1998.

[4] A. Sherwood, M.T Allen, J.R.M.K, Fahrenberg, W. Lovallo, & L. Doornen, "Methodological Guidlines for Impedance Cardiography", Psychophysiology, Vol. 27, No. 1, 1-23. 1990

[5] Y.M Mughal, A. Krivoshei & P. Annus, "Separation of cardiac and respiratory components from the electrical bio-impedance signal using PCA and fast ICA" , Int. Conf. on Control, Eng & Info Tech IPCO. 2013

[6] S. Grimnes, & Ø, G. Martinsen. "Bioimpedance and Bioelectricity Basics", Elsevier. Academic Press 2015

[7] K. Sakamoto, K. Muto, H. Kanai and M. Lizuka, "Problems of impedance cardiography", Med & Biol. Eng. & Comp,17,697-709. 1979

[8] W. Huanli, X. Guizhi, Y. Hongli et al., "Three Dimentional Electrical Impedance Tomography in Thorax Complete Model", 30th Annual IEEE EMBS Conference. British Columbia: pp 466-469, 2008

[9] J. Karnegis, and W. Kubicek, "Physiological correlates of the cardiac thoracic impedance waveform", Am Heart J, vol 79, pp 519-23, 1970

[10] D. Wittoe, and F. Kottke, "The origin of cardiogenic changes in thoracic electrical impedance (del Z)", Feder. Proc; 26, 1967.

[11] K. Baker, D. Hill, and T. Pale, "Comparison of several pulse-pressure tech. for monitoring stroke volume", Med. Biol. Eng.; 12, 81-8, 1974.

[12] W. Kubicek, F. Kottke, M. Ramos, et al., "The Minnesota impedance cardiograph-Theory & appl.",Biomed. Eng, Vol 9, 410-416, 1974.

[13] F. Thompson & A. Joekes, "Thoracic impedance cardiodynamic assessment: Validation in clinical use", London: St. Peter's Hospital, Geigy Pharmaceuticals, 1981.

[14] L. Wang, R. Patterson and B. Raza, "Respiratory effects on cardiac related impedance indices measured under voluntary cardio-respiratory synchronization", Med. Biol. Eng & Comput, vol 29, 505-510, 1991.

[15] R. Patterson, "Source of the thoracic cardiogenic electrical impedance signal as determined by a model", Med & Biol. Eng & Comput, Vol 23, 411-417, 1985.

[16] K. Sakamoto and H. Kania, "Electrical characteristics of flowing blood", IEEE Trans. Biomed. Eng Vol. 26, 686-695, 1979.

[17] R. Lamberts, K. Visser, and W. Zijlstra, "Impedance cardiography", Assen, The Netherlands; Van Gorcum, 1984.

[18] S. Mohapatra, "Noninvasive Cardiovascular Monitoring of Electrical Impedance Technique", London: Pitman, 1981.

[19] B. Penny, "Theory and cardiac applications of electrical impedance measurements", CRC Crit. Rev. Bioeng.; 13, 227-81, 1986.

[20] S. Mohapatra, "Impedance cardiography. In Encyclopedia of Med. Devices and Instrument", NY, pp. 1622-32, John Wiley & Sonss, 1988.

[21] L. Wang, & R. Patterson, "Multiple Source of the Impedance Cardiogram Based on 3-D Finite Difference Human Thorax Models", IEEE Trans. on Biomedical Engineering, Vol. 42, No. 2, 141-148, 1995.

[22] R. Patterson, L. Wang, McWeigh, et al. "Impedance cardiography: The failure of sternal electrodes to predict changes in stroke volume", Biol. Psychol. Vol. 36, pp. 33-41, 1993.

[23] R. Patterson, "Impedance cardiography: What is the source of the signal?", Int. Conf. on Electrical Bioimpedance pp. 1-4, IOP Pub, 2010.

[24] K. Takada, T. Fujinami, K. Senda, & et al., "Clinical study of 'A waves' (atrial waves) in imp. Cardiograms", Am Heart J, 94, 710-7, 1979.

[25] F. Bonjer, J. Berg, MNJ, D. "The origin of the variations of body impedance occuring the cardiac cycle", Circulation, 415-20, 1952.

[26] L. Geddes & L. Baker, "Thoracic impedance changes following saline injection into right & left ventricles", J Appl Physiol, 33, 278-81, 1972.

[27] H. Ito, K. Yamakoshi and A. Yamada, "Physiological and fluid dynamic investigation of the transthoracic impedance plethy.method for measuring cardiac output", Med. Eng Comp; 14, 373-8, 1976.

[28] Y. Saito, T. Goto, and H. Terasaki, "The effects of pulmonary circulation pulsatility on the impedance cardiogram", Arch Internat Physiol Biol; 91, 339-44, 1983.

[29] W. Kubicek, "On the source of peak first time derivative (dZ/dt) during impedance cardiography", Ann of Biomed Eng, 459-62, 1989.

[30] F. Spinal, A. Smith, and F. Crawford, "Relationship of bioimpedance to thermodilution and echocardiographic measurements of cardiac functions", Crit Care Med; 18, 414-8, 1990.

[31] N. Ohashi, Noninvasive estimation of aortic flow by bioelectrical impedance method and its clinical us for assessment of aortic atherosclerosis. Nagoya Med J; 31, 193-207, 1986.

[32] P. Kezakevich, S. Teague and D. Nissman, "Comparative measures of systolic ejection during treadmill exercise by impedance cardiography and Doppler echocardiography", Bio Psychol; 36, 51-61, 1993.

[33] Z. Lababidi, D. Ehmke, and R. Rurnin, "The first derivative thoracic impedance cardiogram", Circulatio; 41, 651-8, 1970.

[34] Y.M. Mughal, "Decomposing of Cardiac and Respiratory Signals from Electrical Bio-impedance Data Using Filtering Method", The Int. Conf. on Health Info. Springer, vol 42, pp 252-255. IFMBE Proc 2013

[35] Y.M. Mughal, Y. Le Moullec, P. Annus and M. Min, "Development of a Bio-Impedance Signal Simulator on the basis of the Regression based Model of the Cardiac and Respiratory Impedance Signals", The 16th Nordic Baltic Conference on Biomedical Engineering and Medical Physics (NBC16), Springer, vol. 48, pages 92-95, IFMBE proc, Gothenburg, Sweden, October 14-16, 2014 .

[36] Da Xu, Kathy L. Ryan, Caroline A. Rickards et al."Improved pulse transit time estimation by system identification analysis of proximal and distal arterial waveforms"American Journal of Physiology - Heart and Circulatory Physiology Published , Vol. 301 no. 4, October 1, 2011